Journal of Materials Science and Engineering A 3 (10) (2013) 678-689

The Role of TiO_2 Anatase Nano-Filler to Enhance the Physical and Electrochemical Properties of PVA-Based Polymer Electrolyte for Magnesium Battery Applications

B.M. Abdel-Samiea[1], A. Basyouni[1], R. Khalil[1,2], Eslam Mohamed Sheha[1], H. Tsuda[3] and T. Matsui[3]

1. Physics Department, Faculty of Science, Benha University, Benha 13518, Egypt

2. Physics Department, Faculty of Science, Tabuk University, KSA

3. Department of Materials Science, Graduate School of Engineering, Osaka Prefecture University, Sakai, Osaka 599-8531, Japan

Received: September 20, 2013 / Accepted: October 02, 2013 / Published: October 10, 2013.

Abstract: The magnesium conducting solid-state polymer electrolyte PE comprising hybrid of poly(vinyl alcohol) (PVA) and magnesium bromide $MgBr_2$, phosphomolbidic acid (PMA) $H_3PMo_{12}O_{40}$, and tetraethylene glycol dimethyl ether (TEGDME) as plasticizer and TiO_2 anatase as a nano-filler is prepared at various compositions by solution cast technique. The interactions between the filler and PE chains are studied by thermal gravimetric analysis (TGA), X-ray diffraction (XRD), scanning electron microscopy (SEM), and impedance spectroscopy. Composition of PE is optimized, and maximum conductivity is obtained at 6 wt.% TiO_2 anatase. Filler seems to increase the number of free magnesium cations by de-coordinating the bond between magnesium cations and matrix scheme. The estimated value of Mg^+ ion transference number is carried out by the combination of complex impedance and D.C. polarization methods and is found to be 0.52 for the highest conducting film. A solid state battery based on the above polymer electrolyte with a configuration Mg|PE|TiO_2 has exhibited a discharge capacity > 8.5 mAh/gm. The discharge characteristics are found to be satisfactory as a laboratory cell.

Key words: Polymer electrolyte, TiO_2 anatase nano-filler, ionic conductivity, magnesium battery.

1. Introduction

Worldwide environmental problems caused by the massive use of fossil fuels demands the search and development of new sources of clean and renewable energy [1]. At the present time, batteries is a steadily growing energy technology and batteries have found markets in variety of applications ranging from consumer electronics and small scale distributed power systems to centralized megawatt scale power plants. In order to be a fully sustainable energy technology, batteries have to qualify in certain indicators of viability such as: Common rechargeable batteries are based on a liquid electrolyte, which implies that there are several restrictions for their design and size due to the available separators and liquid electrolytes. Secondly, these liquid electrolytes carry the inherent risk of leakage. Therefore the need for all-solid-state batteries arises will create more flexibility for the design of stand-alone electronic devices and enhance the applicability in implants due to the avoided leakage risks. The electrolyte loss caused by the leakage and/or volatility of the electrolyte solution has been pointed out to be one of the major problems, which stays the durability of the cell low. In this regard, currently extensive efforts have been dedicated to the research and development of new electrolytes for energy storage cell applications to attain stable and high efficiency performance [2-6].

Rechargeable Mg batteries have shown the potential

Corresponding author: Eslam Mohamed Sheha, associate professor, research field: energy storage. E-mail: ISLAM.SHIHAH@fsc.bu.edu.eg.

for reversible electrochemical energy storage and conversion owing to their characters of high theoretical specific capacity (2,205 $mAhg^{-1}$), great raw material abundance and good operational safety [7, 8]. However, in comparison to Li-ion batteries, the major obstacles for rechargeable Mg batteries are the kinetically sluggish Mg intercalation/insertion and diffusion in cathode materials and the anode/electrolyte incompatibility duo to the high polarizing ability of the divalent Mg^{+2} cation [7-9].

But an important spin-off benefit for the development of Mg-cells may achieve by the emergence of novel alternative materials such as hybrid organic–inorganic nanocomposites are being considered due to their potential for synergic behavior. The combination of polymers and electroactive molecular cluster or extended inorganic species to form nanocomposite hybrid materials represents an opportunity for the design of novel concept materials with improved properties and enhanced energy storage capabilities.

Recently, we reported attempts to construct rechargeable Mg battery systems based on PVA, $MgBr_2$ and phosphomolbidic acid polymer electrolyte and a TiO_2 anatase intercalation cathode [10]. However, much work needs to exploit. Therefore, alternative material families, as well as new design approaches, are highly desirable for ultimate industrialization of Mg secondary batteries.

It has been known that the addition of nanoscale inorganic fillers, such as alumina (Al_2O_3), silica (SiO_2), titania (TiO_2), to the polymer electrolyte resulted in the improvements of transport properties as well as mechanical and electrochemical properties [11-15]. Particularly, the TiO_2 nanoparticles in the polymer electrolyte were confirmed to play useful roles in increasing the ionic conductivity and the cation transference number [16], which were not attributable to the polymer segmental motion but probably to the dipole interaction of TiO_2 with the polymer component [17].

Own to these merits, the present work can tell at least what role or interaction the nano-filler TiO_2 anatase plays in the polymer electrolyte system. From this study, the addition effect of anatase TiO_2 will be also investigated as well as the determination of its optimal content showing the best electrochemical and transport properties. With a polymer electrolyte of optimum composition, solid state Mg/PE/TiO_2 cell is assembled, and its cycling performances will be briefly examined to evaluate the applicability of the polymer electrolyte to solid state rechargeable magnesium batteries.

2. Experiments

2.1 Materials and Preparation

Detailed preparation of polymer electrolyte based Poly (vinyl alcohol), magnesium bromide $MgBr_2$, phosphmolbidic acid (PMA) and TEGDME can be found in our previous paper [10]. Further, Our new electrolyte were developed by adding different amount of TiO_2 anatase nan-filler (x = 2, 4, 6, 8 wt.%).

2.2 Morphology

The morphology of the polymer electrolyte was examined using scanning electron microscope, SEM (JOEL-JSM Model 5600).

2.3 X-Ray Diffraction

The XRD patterns of the films were taken using Rigaku diffractometer type RINT-Ultima IV/S. The diffraction system based with Cu tube anode with voltage 40 kV and current 40 mA.

2.4 Thermogravametric Analysis

Thermogravametric analysis (TGA) was done on a Perkin-Elmer analyzer TGA-7 attached to a professional computer 7700 from room temperature to 200 °C with a heating rate at 10 °C/min.

2.5 Conductivity Measurements

Conductivity measurements were made for PE by

impedance method. Samples of diameter 0.5 cm were sandwiched between the two similar stainless steel electrodes of a spring-loaded sample holder. The whole assembly was placed in a furnace monitored by a temperature controller. The rate of heating was adjusted to be 2 $K \cdot min^{-1}$. Impedance measurements were performed on PM 6304 programmable automatic RCL (Philips) meter in the frequency ranging from 100 Hz to 100 kHz at different temperatures.

2.6 Ionic Transference

Magnesium transference number (t_{Mg}^{+2}) was measured by the steady-state technique which involved a combination of ac and dc measurements. The complex impedance response of the Mg/electrolyte/Mg cell was first measured to determine the cell resistances. It was followed by the dc polarization run, in which a small voltage pulse ($\Delta V = 0.3$ V) was applied to the cell until the polarization current reached the steady-state. Finally, the complex impedance response of the cell was measured a gain to determine the cell resistance after dc polarization.

2.7 Cell Preparation

A powder mixture (0.7 g) of TiO_2 anatase (aldrich anatase < 25 nm), 0.3 gm graphite powder (QualiKems) was thoroughly ground. A slurry obtained by mixing 0.2 gm $MgBr_2$ and 0.1 gm PVA binder using magntic stirrer hot plate (60 ^oC) for 2 hours. To form cathode pellet, the ground powder was mixed with the slurry and left to cast. The electrode is prepared by cold pressing 0.6 gm into a pellet of 13 mm in diameter under 2.5 tons/cm^2. The highest conducting electrolyte is deposited on the cathode substrate using a spin coater at 500 rpm. The anode was prepared by cold pressing 0.6 gm magnesium into a pellet of 13 mm in diameter under 2.5 tons/cm^2. Two-electrodes Swagelok test cell were assembled, Fig. 1, the cell was discharged at room temperature on a multi-channel battery test system (NEWARE BTS-TC35) to analyze the electrochemical responses. The current density was 50 $\mu A/cm^2$.

Elemental mapping and structure of the TiO_2 cathode are measured using wavelength dispersive spectroscopy WDS before and after cycling.

3. Results and Discussion

X-ray diffraction patterns obtained at room temberature for PE containing various wt.% of TiO_2 antase nano-filler are shown in Fig. 2. The patterns show intense peaks at 6.7, 7.73 and 10.8^o which

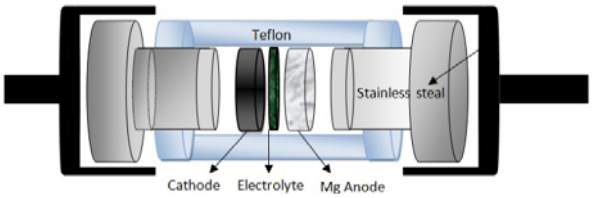

Fig. 1 Schematic design of the lab cell.

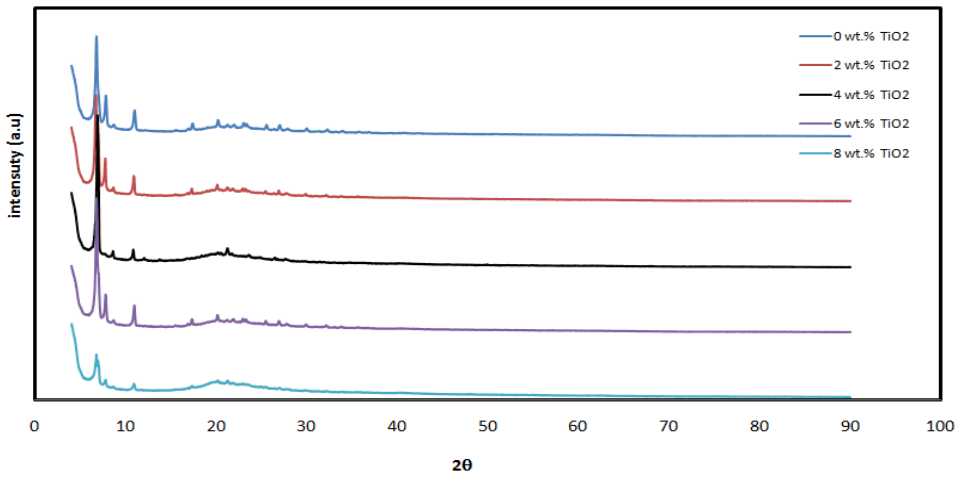

Fig. 2 X-ray diffraction pattern for PE doped with TiO_2 nano-filler.

revealed the crystalline nature of unsolvated acid salt ($H_3PMo_{12}O_{40}$ /$MgBr_2$) in PVA. Furthermore, the broad peak at 20.5° assigned to the semicrystalline nature of O-H ordering of pure PVA bonding scheme [10]. The fact that the intensity of the broad peak has been diminished probably due to the regular incorporation of TiO_2 antase nano-filler into the matrix of polymer host may be due to addition of the filler alters semicrystalline nature of O-H ordering. This relative intensity of broad peak decrease with increase of TiO_2 composition and this may be due to the interaction of the filler with the polymer, resulting in increasing of amorphousity of the system. It is also quite evident that further inclusion of fillers say suggests the presence of some traces of TiO_2 owing to the appearance of additional diffraction peaks at 18°, 21° and 28° which confirms the structure of the complex.

The particle size D of the electrolyte materials was calculated using Scherrer equation as given below [18]:

$$D = 0.9\lambda/(B\cdot\cos\theta)$$

where 0.9 is the Scherrer constant, λ is the wavelength of X-ray, B is the breadth of the pure diffraction profile and θ is the incidence angle of the X-ray. Using this formula, we have calculated the particle size of undoped and TiO_2 doped membrane in the range 16.2-33.2 nm as shown in Table 1.

Scanning electron microscopy (SEM) was used to determine the morphology of the samples. SEM micrographs of hybrid membrane of PE and that doped with TiO_2 anatase nano-filler are shown in Fig. 3. The SEM of pure membrane displays a surface with homogeneous porosity. However, the membrane added with TiO_2 exhibits comparatively compact surface, in which the porosity of the pure membrane disappeared. The disappearance of the porosity is advantageous for interfacial contact between the nano-crystalline TiO_2 filler and electrolyte [19]. On the other hand, for high loading TiO_2 (8 wt.%) a drastic changes in the morphology of the electrolyte and flake-like appearance is clearly seen.

Fig. 4a shows weight loss curves as a function of temperature for PE containing various wt.% of TiO_2 antase nano-filler from room temperature to 400 °C. From Fig. 4a, it is seen that the temperature at which

Table 1 XRD results of PE doped with TiO_2 anatase nano-filler at temperature 30 °C.

TiO_2 wt.%	2θ	d spacing (nm)	FWHM	Particle size (nm)
0	6.75	13.07	0.26	29.79
2	6.67	13.22	0.47	16.81
4	6.87	12.85	0.24	32.15
6	6.75	13.07	0.23	33.20
8	6.73	13.10	0.48	16.25

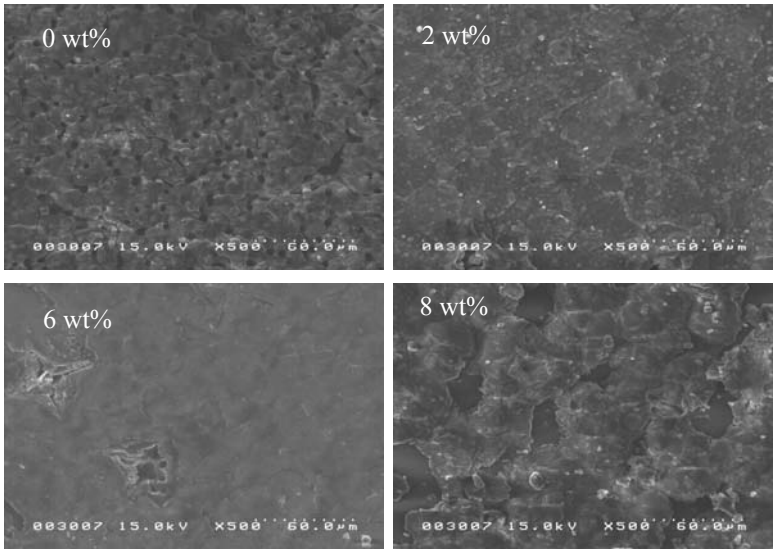

Fig. 3 The SEM for the PE doped with TiO_2 nano-filler.

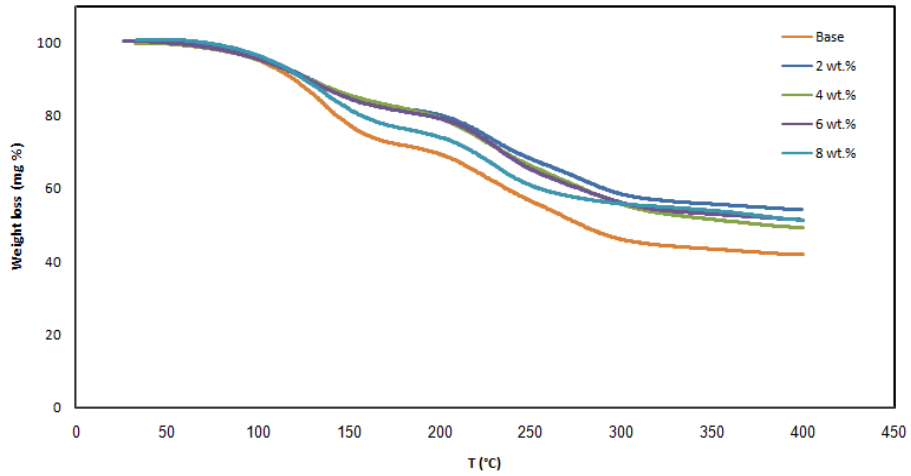

(a)

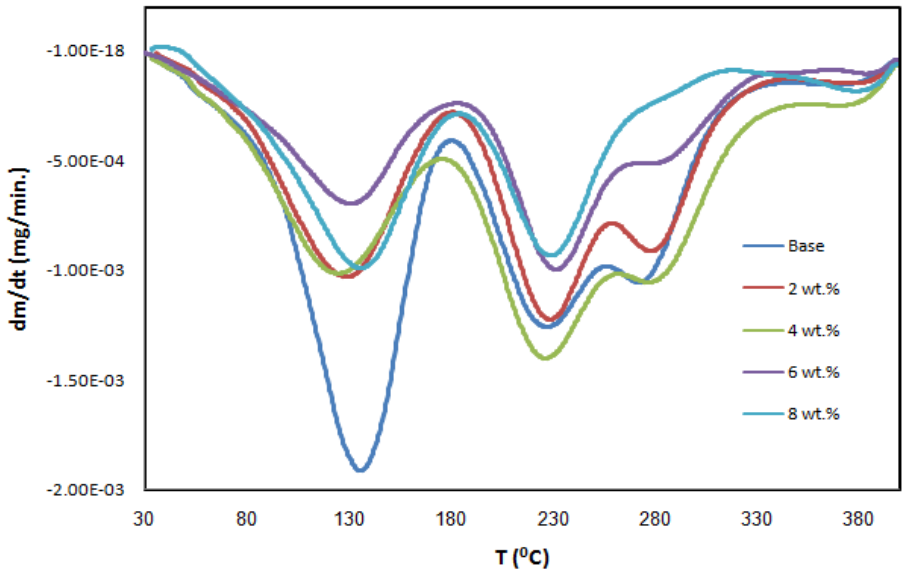

(b)

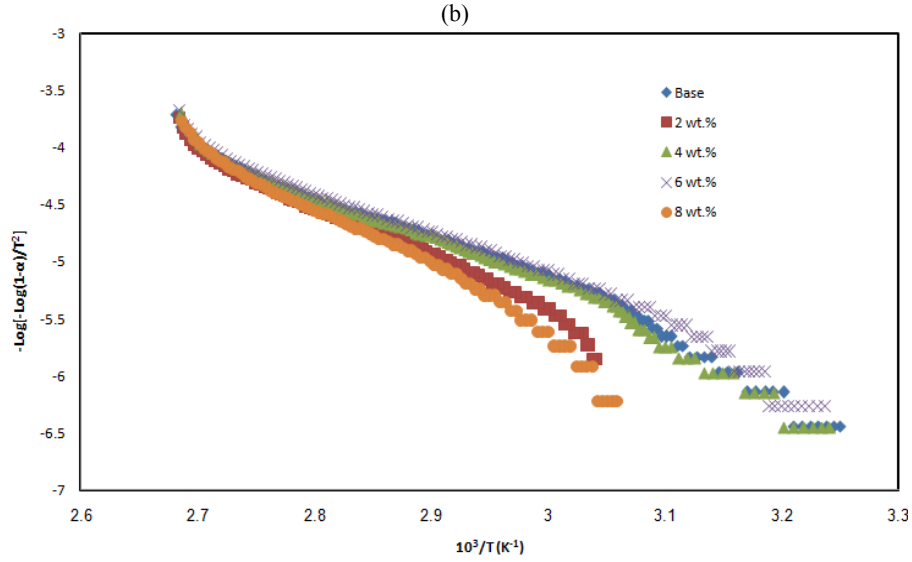

(c)

Fig. 4 TGA curves of untreated and TiO_2 -doped membrane film (a) weight loss against temperature; (b) derivitive of TGA curves and (c) linear plot of TGA curves.

the membranes retained 97 wt.% of their initial weight increased from 88 °C to 96 °C as the doping by TiO_2 nanofillers increased from 0 wt.% to 8 wt.%. This may be attributed to difference in the melting point between PE and filler. In order to ensure the above findings in detail, the drevitive TGA (DrTGA) analysis will be more helpful, Fig. 4b. The glass transition endotherm corresponding to PE is observed at 135.8 °C. The peak position shift to lower temperature with addition of TiO_2 nanofiller content. The occurance of minor shifts in the case of T_m during the inclusion of inorganic fillers tends to explicate the dipole orientation properties of TiO_2 [17, 20, 21]. The low glass transition temperature causes the higher segmental motion of the polymer electrolyte. Such segmental motion produces voids, which enables the easy flow of ions through polymer chains network when there is an applied electric field. The endothermic transformations above 230 °C on DrTGA curve, Fig. 4b, of membranes were due to the structural decomposition of the polymer blends and their complexes. Activation energy for the thermal decomposition of the present samples depends on the residual mass can be calculated using first order integral equation of Coates and Redfern [22, 23]:

$$\log\left[\frac{1-(1-\alpha)}{T^2}\right] = Log\frac{R}{\Delta E_a}\left[1-\frac{2RT}{E_a}\right] - 0.434\frac{E_a}{RT} \quad (1)$$

where, T is the absolute temperature in Kelvin, E_a is the activation energy in J/mol, R is the universal gas constant (8.13 J/mol K) and the fraction of conversion, α, for a weight loss, is given by:

$$\alpha = \frac{w_i - w_a}{w_i - w_f}$$

where w_a , w_i and w_f are the actual, initial and final weight of the samples, respectively.

By plotting the dependence of $-\log\{[-\log(1-\alpha)]/T^2\}$ versus 1,000/T for each sample, we obtain straight lines, Fig. 4c. Then, the apparent activation energies are calculated from the slopes of these lines using the expression:

$$E_a = 2.303R \times \text{slope}$$

Values of the apparent activation energy, Ea, of the samples are listed in Table 2. From this table, it can be observed that the lowest activation energy is for the film doped with 6 and 8 wt.% TiO_2. It is therefore obvious from the present investigation that the best conducting composite polymer electrolyte system having the composition PE/6 and 8 wt.% TiO_2 nanofiller would provide a promising Mg^+ ion conductor for friendly battery applications.

Fig. 5 shows the Cole-Cole plot of PE containing various wt.% of TiO_2 antase nano-filler. The Cole-Cole plot shows semicircle implying that the material is parallel resistive and capacitive. The plot show semicircle diameter decreases with increasing the concentration of TiO_2. The value of R_b (the bulk electrical resistance value) can be calculated from the intercept on the Z' axis. The ionic conductivity can be calculated using equation:

$$\sigma_{dc} = \frac{1}{R} \times \frac{t}{A}$$

where, t is the thickness of the polymer electrolyte film and A is the surface area of the film. The variation in ionic conductivity values for PE/TiO_2 complexes at different TiO_2 content are depicted in Fig. 6. It can be noticed that, the conductivity is not a linear function of the TiO_2 concentration. Thus, a maximum in the conductivity versus composition curve is obtained. The highest ionic conductivity value obtained for this system is at 2.9×10^{-4} S/cm with 6 wt% of TiO_2. The reasons proposed for the enhancement of ionic conductivity, can be attributed to the formation of a new kinetic path via polymer-ceramic boundaries. These boundaries are important because these are the sites for high defect concentration that may allow faster ionic transport. From the above analyses on TiO_2 incorporation in PE system, we can conclude that TiO_2 has brought the conductivity of polymer electrolytes into the useful realm for materials in magnesium polymer battery applications.

Table 2 Electrical and thermal parameters of PE doped with TiO_2 anatase nano-filler.

TiO_2 (wt.%)	E_1 (eV)	E_2 (eV)	n_1	n_2	E_a (kcal·mol^{-1})	Tg (°C)
0.0	0.11	0.11	0.01	0.06	80.4	135.8
2.0	0.10	0.10	0.41	0.53	91.7	128.7
4.0	0.09	0.09	0.21	0.52	84.2	124.5
6.0	0.06	0.06	0.15	0.40	79.03	131.1
8.0	0.14	0.14	0.29	0.36	51.09	135.8

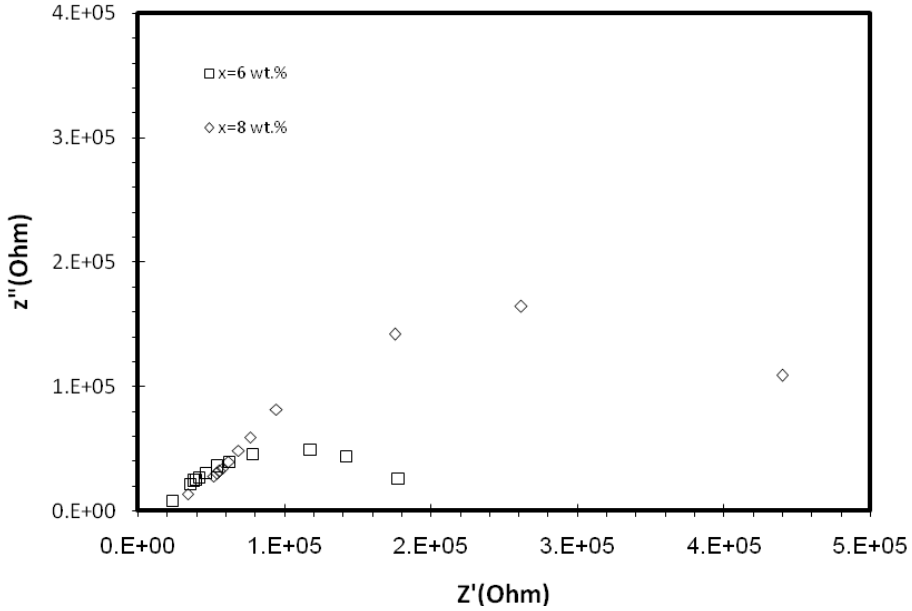

Fig. 5 Cole Cole plots for PE doped with TiO_2 nano-filler.

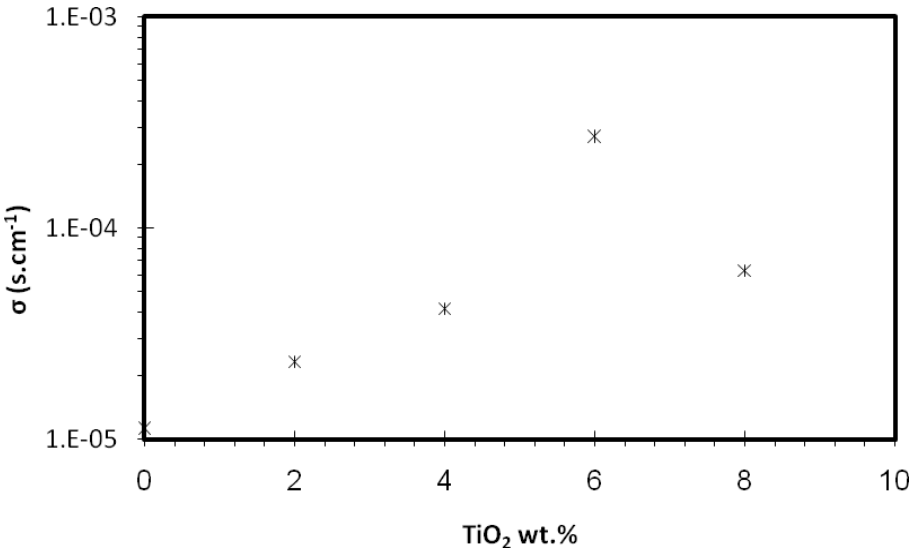

Fig. 6 Variation of ionic conductivity of PE as a function of TiO_2 nano-filler .

Fig. 7 shows the temperature-dependent ionic conductivity of PE containing various wt.% of TiO_2 antase nano-filler. From the plot, it is evident that, as temperature increases the conductivity also increases for all systems. The increase in conductivity with temperature has been explained in terms of segmental motion that result in increasing free volumes of the sample and the motion of ionic charge.

The conductivity can be expressed as the Arrhenius type [24]:

$$\sigma = \sigma_o \exp\left(\frac{-E_a}{KT}\right) \quad (2)$$

where, σ_o in Eq. (2) is a pre-exponential factor, E_a the activation energy, K is the Boltzmann constant and T is the temperature in Kelvins. As shown in Fig. 7, the data are fitted well into two different thermal regions. Table 2 presents the activation energy data; it can be observed that the lowest activation energy is for the film doped with 6 wt.% TiO_2, which indicate that TiO_2 have effect on ionic transfer.

Fig. 8 shows the frequency - dependent conductivity of PE containing various wt.% of TiO_2 antase nano-filler. It seems to follow a universal power law [25]:

$$\sigma_{ac}(\omega) = \sigma_{dc} + A\omega^n \quad (3)$$

where, σ_{dc} is the dc conductivity (the extrapolation of the plateau region to zero frequency), A is the frequency independent pre-exponential factor, ω is the angular frequency and n is the frequency exponent.

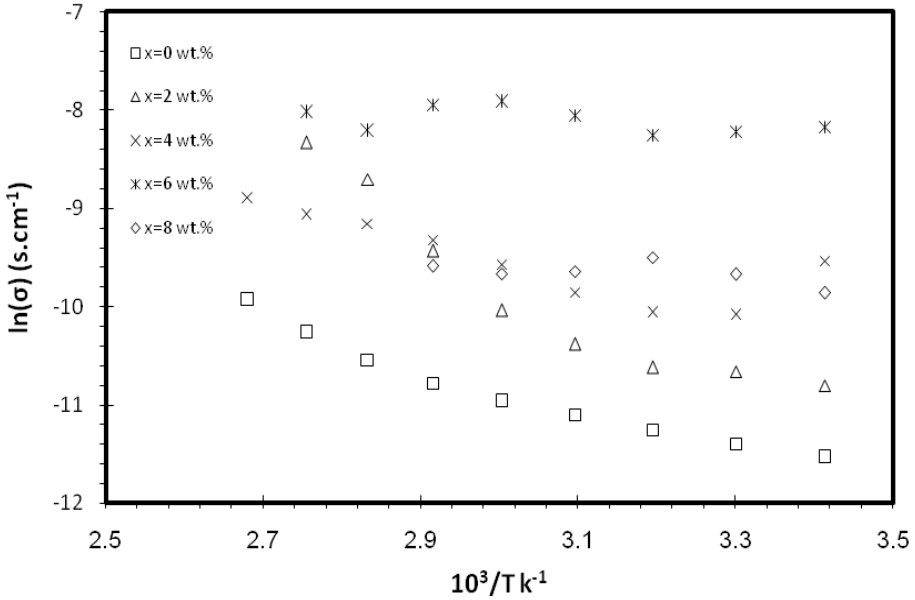

Fig. 7 Temperature dependence of ionic conductivity for PE doped with TiO_2 nano-filler.

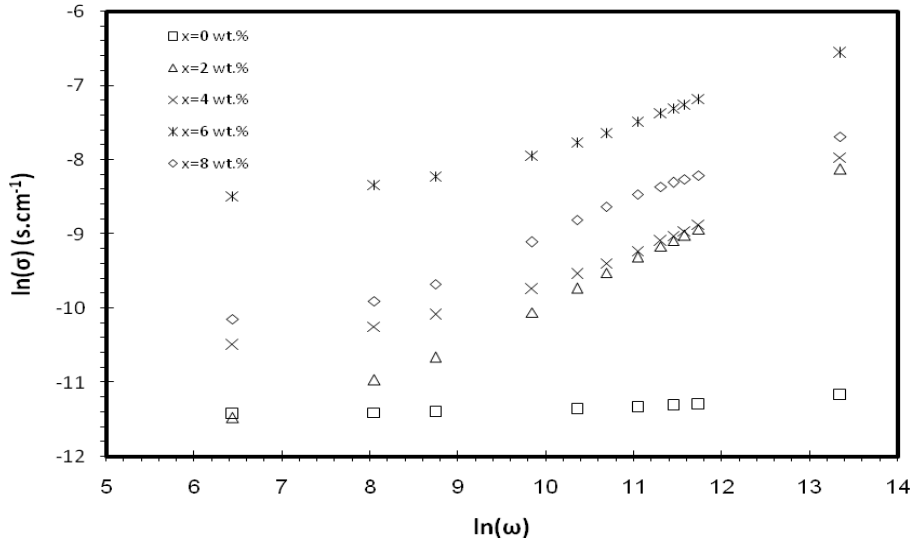

Fig. 8 Frequency dependence of ionic conductivity for PE doped with TiO_2 nano-filler.

The values of the exponent n have been obtained using the least square fitting of Eq. (3) for two regions are listed in Table 2. The values of n lie within the range of $0 < n < 0.5$ for different concentration of TiO_2 anatase nano-filler. The values of n, predicts the domination of hopping conduction in PE/TiO_2 matrix and indicate that the conduction is ionic [26].

The current relaxation curve for the PE doped with TiO_2 antase nano-filler and the impedance spectra was obtained before and after the polarization of Mg/PE/Mg cell, Fig. 9. The Magnesium transference number t_{mg}^{2+} was measured by the following equation [27]:

$$t_{mg^{2+}} = \frac{I_s(\Delta V - R_o I_o)}{I_o(\Delta V - R_s I_s)} \quad (4)$$

where, I_o and I_s are the initial and final steady-state currents and R_0 and R_s are the cell resistances before and after the polarization, respectively. The value of Magnesium transference number t_{mg}^{2+} was estimated by 0.529 at room temperature.

The film with the highest electrical conductivity was used for cell fabrication. Fig. 10a shows charge-discharge curves of Mg/TiO_2 battery. the cells was discharged at a constant current density of 50 μA/cm^2 at room temperature. The discharge curves of Mg/TiO_2 cell displayed activation of discharge voltage, This suggests that activation of electrode surface took place during the initial charge / discharge cycling [28]. Fig. 10b shows the complete discharge curve of the battery, It shows that the discharge was sustained for 150 h. The value of the discharge capacity C was evaluated from the equation [2]:

$$C = \int_0^t I(t)dt \quad (5)$$

by integrating the area under the curve of Fig. 10b. The discharge capacity was estimated by 8.5 mAh.

WDS results of TiO_2 cathode before and after cycling are shown in Table 3. The results indicate that the ratio of the Mg^+ to Ti^+ ions increased after cycling than before. This means that the electrolyte allows the flow of Mg^+ ions, from Mg anode to TiO_2 cathode.

X-ray diffraction patterns of TiO_2 cathode before and after cycling are shown in Fig. 11. It is clearly observed that the entire fingerprint peaks, viz. 25.2 (TiO_2 [29]) and 26.5° (graphite [2]) suggesting the existence of TiO_2/graphite structure. The change in the intensity and position values of the fingerprint peak (2θ = 25.2°) before and after cycling can be attributed to the substitution of Mg^+ with Ti^+ ions and this agrees with the WDS results. The process of charging and

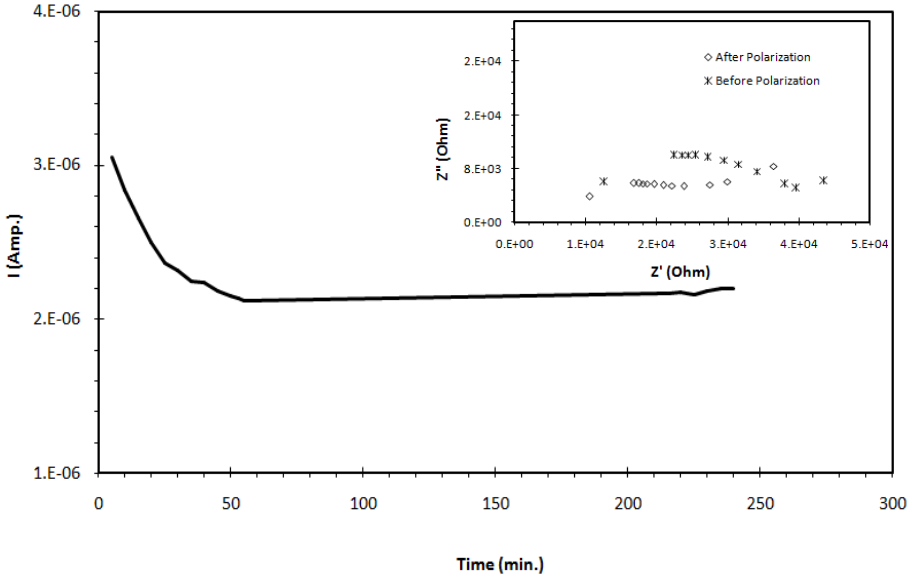

Fig. 9 The variation of polarization current as a function of time for PE doped with TiO_2 nano-filler.

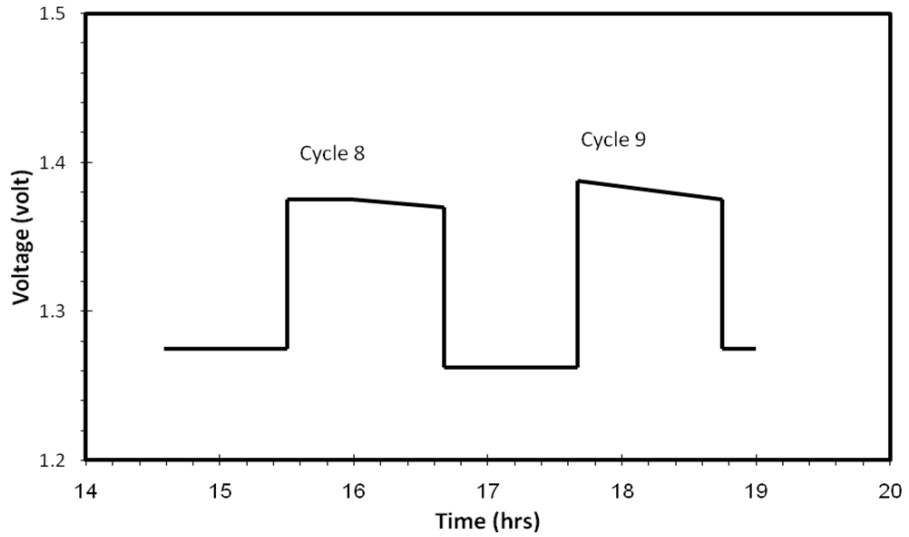

(a)

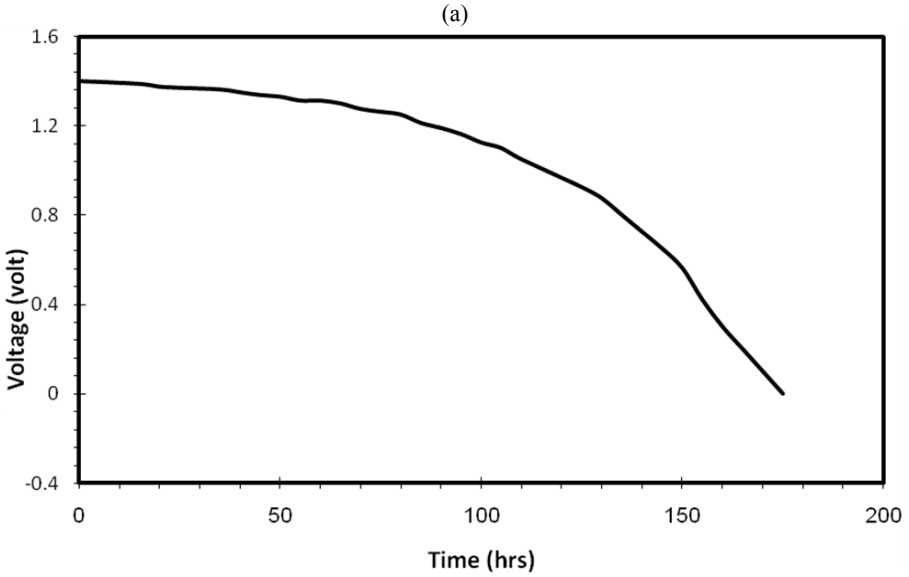

(b)

Fig. 10 Discharge charactristics of TiO_2 cathode (a) charge-discharge cycles and (b) complete discharge curve.

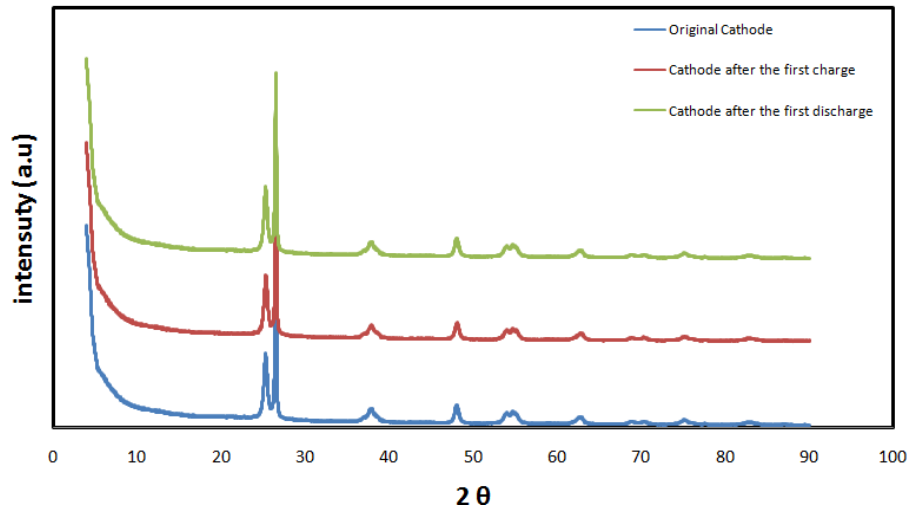

Fig. 11 XRD pattern of TiO_2 electrodes before and after charge-discharge.

Table 3 WDS results of TiO_2 cathode before and after cycling.

Cathode status	TiO_2 cathodes (Mg/Ti) ratio (wt.%)
Original cathode	0.14
After the first discharge	0.22
After the first charge	0.28

Table 4 XRD results of TiO_2 cathode before and after cycling.

Cathode status	2Theta	d	FWHM	Particle size (nm)
Original cathode	25.32	3.5138	0.50	16.27
After the first discharge	25.30	3.5172	0.50	16.22
After the first charge	25.33	3.5129	0.50	16.18

discharging of these batteries involves the insertion of ions into both positive and negative electrodes. In these batteries, the Mg ion shuttles between the positive and the negative electrode, as lithium ions in lithium batteries.

The particle size of the cathode was calculated using Scherer equation, Table 4. The particle size ranged from 16.27 to 16.18 nm before and after cycling, respectively. This reduction in the crystallite size can be attributed to the strain experienced due to intercalation and de- intercalation of Mg^{+2} as follow:

$$TiO_2 + {}_xMg^{+2} + {}_xe^- \leftrightarrow Mg_xTiO_2$$

4. Conclusions

The ionic conductivity depended on the content of TiO_2. The highest conductivity of the PE examined was ~10^{-5} S/cm (at 30 °C) for the composition of 6 wt.% TiO_2. The enhancement in ionic conductivity when adding TiO_2 filler to a PVA-Mg acid salt complex might be due to the fact that the active dissociation of the Mg salt results in an increased concentration of mobile carriers. WDS and X-ray study of the cathodes before and after discharge show that the electrolyte allows the flow of Mg ions.

Acknowledgments

The authors are grateful to the Science technology development fund of Egypt, grant number 2069. Also a lot of thanks are due to Dr. Tsunekane and Messrs. Toko, Tohki and Koide for their help at Osaka Prefecture University.

References

[1] S. Anandan, R. Sivakumar, Effect of loaded TiO_2 nanofiller on heteropolyacid-impregnated PVDF polymer electrolyte for the performance of dye-sensitized solar cells, Phys. Status Solid A (2009) 206-343.

[2] E. Sheha, Ionic conductivity and dielectric properties of plasticized $PVA_{0.7}(LiBr)_{0.3}(H_2SO_4)_{2.7M}$ solid acid membrane and its performance in a magnesium battery, Solid State Ionics 180 (2009) 1575-1579.

[3] T. Kuila, H. Acharya, S.K. Srivastava, B.K. Samantaray, S. Kureti, Enhancing the ionic conductivity of PEO based plasticized composite polymer electrolyte by $LaMnO_3$ nanofiller, Mater. Sci. Eng. 107 (2007) 217-224.

[4] Y. Li, J.W. Wang, J.W. Tang, Y.P. Liu, Y.D. He, Conductive performances of solid polymer electrolyte films based on PVB/$LiClO_4$ plasticized by $PEG_{200,}PEG_{400}$ and PEG_{600}, J. Power Sources 187 (2009) 305-311.

[5] G.P. Pandey, R.C. Agrawal, S.A. Hashmi, Magnesium ion-conducting gel polymer electrolytes dispersed with nanosized magnesium oxide, J. Power Sources 190 (2009) 563-572.

[6] S.A. Suthanthiraraj, S.D. Joice, P.B. Joseph, Impact of ethylene carbonate on ion transport characteristics of PVdF-$AgCF_3SO_3$ polymer electrolyte system, Mater. Research Bulletin140 (2009) 1534-1539.

[7] W. Li, C. Li, C. Zhou, H. Ma, J. Chen, Metallic magnesium nano/mesoscale structures: Their shape-controlled preparation and Mg/Air battery applications, Angewandte. Chemie. 118 (2006) 6155-6158.

[8] Y. Liang, R. Feng, S. Yang, H. Ma, J. Liang, J. Chen, Rechargeable Mg Batteries with graphene-like MoS_2 cathode and ultrasmall Mg nanoparticle anode, Adv. Mater. 23 (2011) 640-643.

[9] D. Aurbach, Z. Lu, A. Schechter, Y. Gofer, H. Gizbar, R. Turgeman, et al., Prototype systems for rechargeable magnesium batteries, Nature 407 (2000) 724-727.

[10] E. Sheha, Prototype system for magnesium/TiO_2 anatase batteries, Int. J. Electrochem. Sci. 8 (2013) 3653-3663.

[11] K.M. Kim, K.S. Ryu, S.G. Kang, S.H. Chang, I.J. Chung, The effect of silica addition on the properties of Poly((vinylidene fluoride)-co-hexafluoropropylene)-based polymer electrolytes, Macromol. Chem. Phys. 2002 (2001) 866-872.

[12] K.M. Kim, N.G. Park, K.S. Ryu, S.H. Chang, Characterization of poly(vinylidenefluoride-co-

hexafluoropropylene)-based polymer electrolyte filled with TiO_2 nanoparticles, Polymer 43 (2002) 3951-3957.

[13] F. Croce, G.B. Appetecchi, L. Persi, B. Scrosati Nanocomposite polymer electrolytes for lithium batteries, Nature 394 (1998) 456-458.

[14] B. Scrosati, F. Croce, L. Persi, Impedance spectroscopy study of PEO-based nanocomposite polymer electrolytes, J. Electrochem. Soc. 147 (2000) 1718-1721.

[15] Y. Aihara, G.B. Appetecchi, B. Scrosati, K. Hayamizu Investigation of the ionic conduction mechanism of composite poly(ethyleneoxide) PEO-based polymer gel electrolytes including nano-size SiO_2, Phys. Chem. Chem. Phys. 4 (2002) 3443-3447.

[16] S.H. Chung, Y. Wang, L. Persi, F. Croce, S.G. Greenbaum, B. Scrosati, et al., Enhancement of ion transport in polymer electrolytes by addition of nanoscale inorganic oxides, J. Power Sources 97-98 (2001) 644-648.

[17] B. Kumar, L.G. Scanlon, R.J. Spry on the origin of conductivity enhancement in polymer-ceramic composite electrolytes, J. Power Sources 96 (2001) 337-342.

[18] S. Kitazawa, Y. Choi, S. Yamamoto, T. Yamaki, Rutile and anatase mixed crystal TiO_2 thin films prepared by pulsed laser deposition, Thin Solid Films 515 (2006) 1901-1904.

[19] H.W. Han, W. Liu, J. Zhang, X.Z. Zhao, A Hybrid poly(ethylene oxide)/poly(vinylidene fluoride)/TiO_2 nanoparticle solid-state redox electrolyte for dye-sensitized nanocrystalline solar cells, Adv Func. Mater. 15 (2005) 1940-1944.

[20] M. Johnsi, S. Austin, Synthesis and characterization of a new composite polymer electrolyte based on Al_2O_3 nanofiller, Int. J. Chem. Environ. & Tech. 1 (2013) 12-21.

[21] S. Ramesh, K. Ramesh, A.K. Arof, Fumed silica-doped poly(vinyl chloride)-poly(ethylene oxide) (PVC/PEO)-based polymer electrolyte for lithium ion battery, Int. J. Electrochem. Sci. 8 (2013) 8348-8355.

[22] E.M. Abdelrazek, I.S. Elashmawi, A. El-khodary, A. Yassin, Structural, optical, thermal and electrical studies on PVA/PVP blends filled with lithium bromide, Curr. Appl. Phys. 10 (2010) 607-613.

[23] S. Badr, E. Sheha, Impact of hydroquinone on thermal and electrical properties of plasticized [poly (vinyl alcohol)]$_{0.7}$(LiBr)$_{0.3}$(H_2SO_4) 2.9 mol·L^{-1} solid acid membrane, Polym. Int. 60 (2011) 1142-1148.

[24] M. Watanabe, K. Sanui, N. Ogata, T. Kobayashi, Z. Ohtaki, Ionic conductivity and mobility in network polymers from poly(propylene oxide) containing lithium perchlorate, J. Appl. Phys. 57 (1985) 123-128.

[25] M.H. Harun, E. Saion, A. Kassim, M.Y. Hussain, I.S. Mustafa, M.A.A. Omer, Temperature dependence of ac electrical conductivity of PVA-PPy-$FeCl_3$ composite polymer films, Malays. Polym. J. (MPJ) 3 (2008) 24-31.

[26] F.H. Abd El-kader, H.W. Osman, K.H. Mahmoud, M.A.F. Basha, Dielectric investigations and ac conductivity of polyvinyl alcohol films doped with europium and terbium chloride, Physica B 403 (2008) 3473-3484.

[27] G.P. Pandey, R.C. Agrawal, S.A. Hashmi, Magnesium ion conducting gel polymer electrolytes dispersed with fumed silica for rechargeable magnesium battery application, J. Solid State Electrochemistry 15 (2011) 2253-2264.

[28] A.A. Mohamad, N.S. Mohamed, Y. Alias, A.K. Arof, Studies of alkaline solid polymer electrolyte and mechanically alloyed polycrystalline Mg2Ni for use in nickel metal hydride batteries, Journal of Alloys and Compounds 337 (1) (2002) 208-213.

[29] H.C. Tao, L.Z. Fan, X. Yan, X. Qu, In situ synthesis of TiO_2-graphene nanosheets composites as anode materials for high-power lithium ion batteries, Electrochimica Acta 69 (2012) 328-333.